Sparse Regression Incorporating Graphical Structure Among Predictors

Guan Yu & Yufeng Liu

Taylor & Francis
Taylor & Francis Group

Sparse Regression Incorporating Graphical Structure Among Predictors

Guan Yu and Yufeng Liu

ABSTRACT

With the abundance of high-dimensional data in various disciplines, sparse regularized techniques are very popular these days. In this article, we make use of the structure information among predictors to improve sparse regression models. Typically, such structure information can be modeled by the connectivity of an undirected graph using all predictors as nodes of the graph. Most existing methods use this undirected graph edge-by-edge to encourage the regression coefficients of corresponding connected predictors to be similar. However, such methods do not directly use the neighborhood information of the graph. Furthermore, if there are more edges in the predictor graph, the corresponding regularization term will be more complicated. In this article, we incorporate the graph information node-by-node, instead of edge-by-edge as used in most existing methods. Our proposed method is very general and it includes adaptive Lasso, group Lasso, and ridge regression as special cases. Both theoretical and numerical studies demonstrate the effectiveness of the proposed method for simultaneous estimation, prediction, and model selection. Supplementary materials for this article are available online.

1. Introduction

Linear regression plays a fundamental role in statistics. It is widely used in many different scientific areas. Under the standard setting with the sample size n larger than the dimension p, the commonly used ordinary least squares (OLS) estimator for the p-dimensional coefficient vector β^0 often works well. On the other hand, it is also well known that OLS often leads to complicated models with low prediction accuracy when the predictors are highly correlated. Furthermore, for the high-dimensional data ($p \gg n$), OLS is not applicable due to the rank deficiency of the design matrix. To improve OLS, many penalized methods using regularization in model fitting have been proposed in the literature. For example, classical ridge regression (Hoerl and Kennard 1970) uses the ridge penalty $\sum_{i=1}^{p} |\beta_i^0|^2$ to achieve better prediction performance through a bias–variance tradeoff. The popular Lasso method (Tibshirani 1996) uses the l_1 penalty $\sum_{i=1}^{p} |\beta_i^0|$ to perform continuous shrinkage and automatic variable selection simultaneously. It is known from the literature that Lasso has many good theoretical properties such as model selection consistency (Zhao and Yu 2006), estimation consistency (Knight and Fu 2000), and persistence property for prediction (Greenshtein 2006). However, Lasso also has some limitations. For example, the shrinkage introduced by Lasso results in significant bias toward 0 for large regression coefficients (Fan and Li 2001). In the presence of some highly correlated variables, Lasso tends to select only one of those variables (Zou and Hastie 2005).

Besides the Lasso, a lot of other penalized methods have been proposed for simultaneous variable selection and estimation. For example, Fan and Li (2001) introduced the smoothly clipped absolute deviation (SCAD) method. Zou and Hastie (2005)

proposed the elastic net method and Zou (2006) proposed the adaptive Lasso estimator. Wang, Li, and Jiang (2007) use the least absolute deviation Lasso for robust regression. Liu and Wu (2007) used a new penalty that combines the l_0 and l_1 penalties. Witten and Tibshirani (2009) proposed the scout method which includes many penalized methods as special cases. Zhang (2010) studied the minimax concave penalty (MCP) which is a nearly unbiased method for penalized variable selection.

Despite the vast literature on sparse regression, few methods use the structure information of the predictors which can be modeled by the connectivity of an undirected graph. It would be very interesting and useful to study how to use this structure information to improve the performance of variable selection, estimation, and prediction. In general, we can get the structure information of the predictors from prior information or estimation. For example, many biological studies have shown that there may exist some regulatory relationships between genes (Li and Li 2008). An increasing amount of information about gene interaction is organized in databases (Subramanian et al. 2005). This biological information can be used to construct the predictor graph where nodes represent genes and edges indicate regulatory relationships. If the prior information is not available in some applications, we can construct the predictor graph by sparse estimation of the covariance (or precision) matrix of the predictors (Yuan and Lin 2007; Friedman, Hastie, and Tibshirani 2008; Cai, Liu, and Luo 2011).

Since the predictor graph cannot be represented as some nonoverlapping groups, the traditional group Lasso method (Yuan and Lin 2006) cannot make full use of this complicated structure information. To use the entire predictor graph infor-

CONTACT Yufeng Liu ✉ yfliu@email.unc.edu 🖳 Department of Statistics and Operations Research and Department of Genetics, Carolina Center for Genome Sciences, Department of Biostatistics, University of North Carolina at Chapel Hill, NC 27599

Color versions of one or more of the figures in the article can be found online at www.tandfonline.com/r/JASA.

🅑 Supplementary materials for this article are available online. Please go to www.tandfonline.com/r/JASA

mation, most existing methods use the graph edge-by-edge, through adding some penalty terms to encourage coefficients β_i^0 and β_j^0 to be similar for predictors i and j connected by an edge. One type of methods encourages β_i^0 and β_j^0 to be zero or nonzero simultaneously. For example, OSCAR (Bondell and Reich 2008) uses the l_∞ penalty $\max\{|\beta_i^0|, |\beta_j^0|\}$ for every pair of different predictors. Yang et al. (2012) generalized OSCAR to graph OSCAR (GOSCAR) which only uses the l_∞ penalty for those pairs of predictors connected by an edge in the given predictor graph. Pan, Xie, and Shen (2010) introduced a weighted L_γ-regularization. Kim, Pan, and Shen (2013) proposed a new nonconvex penalty term based on the truncated lasso penalty. Another type of methods uses some penalty terms to encourage β_i^0 and β_j^0 to have similar values or absolute values. For example, GRACE (Li and Li 2008) uses the penalty $(\beta_i^0/\sqrt{d_i} - \beta_j^0/\sqrt{d_j})^2$ to smooth the weighted β_i^0 over the predictor graph, where d_i is the degree of predictor i. GFlasso (Kim and Xing 2009) uses the penalty $|\beta_i^0 - \mathrm{sign}(\hat{\rho}_{ij})\beta_j^0|$ where $\hat{\rho}_{ij}$ is the sample correlation coefficient between predictors i and j. Zhang et al. (2013) proposed the logistic graph Laplacian net. Other methods of this type include Yang et al. (2012) and Zhu, Shen, and Pan (2013) which use some nonconvex penalty terms to encourage $|\beta_i^0|$ and $|\beta_j^0|$ to be similar. Although penalized methods using the predictor graph edge-by-edge are promising in improving regression performance, they also have some drawbacks. On the one hand, these methods do not directly use the neighborhood information of the graph. For each neighborhood, it can be preferable to use the corresponding edges jointly rather than separately. On the other hand, the penalty terms in these methods will be more complicated if there are more edges in the graph.

In this article, instead of using the predictor graph *edge-by-edge*, we propose a new method, namely Sparse Regression Incorporating Graphical structure among predictors (SRIG), using the graph *node-by-node*. Specifically, according to the predictor graph G, we assume that there is a latent decomposition of β^0 into p parts $V^{(1)}, V^{(2)}, \ldots, V^{(p)}$ such that $\beta^0 = \sum_{i=1}^{p} V^{(i)}$ and each $V^{(i)} \in R^p$. The proposed SRIG imposes a penalty to shrink some V_i to 0 while the other V_i's satisfy $\mathrm{supp}(V_i) = \mathcal{N}_i$, where $\mathcal{N}_i$ is a set including predictor i and its neighbors in graph G. For SRIG, if one predictor is important for prediction, the other predictors connected to it are also encouraged to be in the model. Note that our proposed SRIG method is a graph-based penalized regression method with a very different motivation, although the corresponding optimization problem can be formulated as a special case of the latent group Lasso approach (Obozinski, Jacob, and Vert 2011) with each neighborhood $\mathcal{N}_i$ as a group. For computation, besides introducing the predictor duplication method shown in Obozinski, Jacob, and Vert (2011), we also propose a new iterative proximal algorithm which is very efficient for high-dimensional data. Our theoretical study shows that SRIG has close connections with several existing methods: (1) It is the same as the adaptive Lasso method when the predictor graph G has no edge; (2) It is equivalent to the group Lasso method when G consists of multiple complete subgraphs; (3) It has the same nonzero solution set as the ridge regression when G is a complete graph. Under some conditions, SRIG enjoys model selection consistency and acquires tight finite sample bounds for both estimation and

prediction. To evaluate the performance of SRIG, we compare SRIG with many existing methods. Simulation examples with different kinds of predictor graphs are studied. We also analyze a dataset from the Alzheimer's Disease Neuroimaging Initiative (ADNI) database (*www.loni.ucla.edu/ADNI*). The structural magnetic resonance imaging (MRI) features are used to predict the mini-mental state examination (MMSE) score (Folstein, Folstein, and McHugh 1975). Both the simulation results and the real data application indicate that SRIG has competitive performance in estimation, prediction, and model selection.

The rest of the article is organized as follows. In Section 2, we motivate and introduce our proposed SRIG method. In Section 3, we introduce two methods to solve the optimization problem. In Section 4, we show some theoretical properties. In Sections 5 and 6, we demonstrate the use of SRIG on simulated data and the ADNI dataset. We conclude this article with some discussion in Section 7. Technical proofs are provided in the supplementary materials.

2. Motivation and Methodology

Consider the following linear regression model:

$$Y = X\beta^0 + \epsilon, \tag{1}$$

where $\epsilon = (\epsilon_1, \epsilon_2, \ldots, \epsilon_n)^T$ is a vector of iid random variables with mean 0 and variance σ^2. Here, $\beta^0 = (\beta_1^0, \beta_2^0, \ldots, \beta_p^0)^T$ is a vector of true coefficients, $Y = (y_1, y_2, \ldots, y_n)^T$ is an $n \times 1$ response, and $X = (X_1, X_2, \ldots, X_p) = (x_1, x_2, \ldots, x_n)^T$ is an $n \times p$ design matrix.

For motivation, we first consider the random design setting and assume that each x_k follows some multivariate distribution with mean $0_{p \times 1}$ and covariance matrix Σ. The design matrix X is assumed to be independent of the random error ϵ. Furthermore, denote $\Omega = (\omega_{ij})_{i,j=1,2,\ldots,p} = \Sigma^{-1}$ and $\Sigma_{xy} = (c_1, c_2, \ldots, c_p)^T \in R^p$ as the cross-covariance vector between x_k and y_k.

By model (1) and the definition of cross-covariance, we have

$$\Sigma_{xy} = E(X^T Y/n) = E(X^T X\beta^0/n) + E(X^T \epsilon/n) = \Sigma\beta^0.$$

Then, we observe that $\beta^0 = \Sigma^{-1}\Sigma_{xy} = \Omega\Sigma_{xy}$, where Ω measures partial correlations among predictors, and Σ_{xy} reflects the marginal correlations between predictors and response variable. From $\beta^0 = \Omega\Sigma_{xy}$, we have

$$\beta_1^0 = c_1\omega_{11} + c_2\omega_{12} + \cdots + c_i\omega_{1i} + \cdots + c_p\omega_{1p}$$
$$\beta_2^0 = c_1\omega_{21} + c_2\omega_{22} + \cdots + c_i\omega_{2i} + \cdots + c_p\omega_{2p}$$
$$\vdots$$
$$\beta_p^0 = c_1\omega_{p1} + c_2\omega_{p2} + \cdots + c_i\omega_{pi} + \cdots + c_p\omega_{pp}.$$

Note that β^0 is the sum of p parts, $\{(c_i\omega_{1i}, c_i\omega_{2i}, \ldots, c_i\omega_{pi})^T : 1 \le i \le p\}$. For the ith part, $(c_i\omega_{1i}, c_i\omega_{2i}, \ldots, c_i\omega_{pi})^T$, there is a common factor c_i. If the ith predictor and the response variable are uncorrelated marginally, then c_i will be 0 and all the components in the ith part of β^0 will be 0 simultaneously. Furthermore, if c_i is not zero and the predictor graph is defined by Ω, then the support of $(c_i\omega_{1i}, c_i\omega_{2i}, \ldots, c_i\omega_{pi})^T$ becomes $\mathcal{N}_i$, which is a set including predictor i and its neighbors in the predictor

graph. Thus, instead of focusing on β^0 in the model, we consider a latent decomposition of β^0 into p parts. After choosing the candidate nonzero components in each part based on $\mathcal{N}_1, \mathcal{N}_2, \ldots, \mathcal{N}_p$, we use the group sparsity constraint to encourage the selected components in each part to be zero or nonzero simultaneously.

The above idea can be generalized for an arbitrary predictor graph constructed by the prior information or estimation from data. Given the predictor graph G, we define a $p \times p$ adjacency matrix E, where $E_{ij} = 1$ if predictors i and j are connected and $E_{ij} = 0$ otherwise. For each i, we set $E_{ii} = 1$ and acquire the neighborhood set $\mathcal{N}_i = \{j : E_{ij} = 1\}$. As the previous case, we assume that β^0 can be decomposed into

$$\beta_1^0 = V_1^{(1)}E_{11} + V_1^{(2)}E_{12} + \cdots + V_1^{(i)}E_{1i} + \cdots + V_1^{(p)}E_{1p}$$
$$\beta_2^0 = V_2^{(1)}E_{21} + V_2^{(2)}E_{22} + \cdots + V_2^{(i)}E_{2i} + \cdots + V_2^{(p)}E_{2p}$$
$$\vdots$$
$$\beta_p^0 = V_p^{(1)}E_{p1} + V_p^{(2)}E_{p2} + \cdots + V_p^{(i)}E_{pi} + \cdots + V_p^{(p)}E_{pp}.$$

Here, the ith part is $(V_1^{(i)}E_{1i}, V_2^{(i)}E_{2i}, \ldots, V_p^{(i)}E_{pi})^T$ whose candidate nonzero components are $\{V_j^{(i)}E_{ji} : j \in \mathcal{N}_i\}$. We can view $\{V_j^{(i)} : j \in \mathcal{N}_i\}$ as the effect arising from the marginal correlation between the ith predictor and the response variable. If they are uncorrelated, $V_j^{(i)}$ will be zero for each $j \in \mathcal{N}_i$ and the components in the set $\{V_j^{(i)}E_{ji} : j \in \mathcal{N}_i\}$ will be zero simultaneously. Therefore, after choosing the candidate nonzero components in each part based on $\mathcal{N}_1, \mathcal{N}_2, \ldots, \mathcal{N}_p$, it is reasonable to use the group sparsity constraint to encourage the selected components in each part to be zero or nonzero together. Based on this motivating idea, given the training data (Y, X) and predictor graph G, we propose a new method, Sparse Regression Incorporating Graphical structure among predictors (SRIG), shown as follows.

SRIG Method

Step 1. Find the neighborhoods $\mathcal{N}_1, \mathcal{N}_2, \ldots, \mathcal{N}_p$ (note that $i \in \mathcal{N}_i$ for each i).
Step 2. Solve the following optimization problem:

$$\min_{\beta, V^{(1)}, \ldots, V^{(p)}} \frac{1}{2n}\|Y - X\beta\|_2^2 + \lambda \sum_{i=1}^{p} \tau_i \|V^{(i)}\|_2, \qquad (2)$$

subject to $\sum_{i=1}^{p} V^{(i)} = \beta$ and $\text{supp}(V^{(i)}) \subseteq \mathcal{N}_i$ for each i, where $\text{supp}(V^{(i)})$ is the support of vector $V^{(i)}$ and $\|\cdot\|_2$ is the l_2 norm.

Here, we use τ_i to denote the positive weight for the ith group. The choice of τ_i will be discussed in Section 4.4.

3. Computation

In this section, we introduce two methods to solve the problem (2). One is the predictor duplication (PD) method proposed in Obozinski, Jacob, and Vert (2011) and another one is our proposed iterative proximal (IP) algorithm. The predictor duplication method transforms (2) to a traditional group Lasso problem by duplicating predictors while our proposed new algorithm solves problem (2) directly without duplicating predictors.

3.1 Predictor Duplication Method

Denote $V_{\mathcal{N}_i}^{(i)}$ as the $|\mathcal{N}_i| \times 1$ sub-vector of $V^{(i)}$ with indices in $\mathcal{N}_i$ and $X_{\mathcal{N}_i}$ as the $n \times |\mathcal{N}_i|$ submatrix of X with column indices in $\mathcal{N}_i$. Denote $\tilde{V} = (V_{\mathcal{N}_1}^{(1)T}, V_{\mathcal{N}_2}^{(2)T}, \ldots, V_{\mathcal{N}_p}^{(p)T})^T$ and $\tilde{X} = (X_{\mathcal{N}_1}, X_{\mathcal{N}_2}, \ldots, X_{\mathcal{N}_p})$. Then, we can check that $X\beta = \tilde{X}\tilde{V}$, and problem (2) is equivalent to the following group Lasso problem:

$$\min_{\tilde{V}} \frac{1}{2n}\|Y - \tilde{X}\tilde{V}\|_2^2 + \lambda \sum_{i=1}^{p} \tau_i \|V_{\mathcal{N}_i}^{(i)}\|_2. \qquad (3)$$

Many efficient R packages such as `grpreg` (Breheny and Huang 2009) and `gglasso` (Yang and Zou 2013) can be used to solve problem (3). After setting $\hat{V}_{\mathcal{N}_i^c}^{(i)} = 0$ for each i, we have $\hat{\beta} = \sum_{i=1}^{p} \hat{V}^{(i)}$. Note that in some cases, some neighborhoods $\{\mathcal{N}_i : i \in F\}$ maybe exactly the same. Then, the vectors $\{V_{\mathcal{N}_i}^{(i)} : i \in F\}$ are indistinguishable and therefore the decomposition of β (i.e., $\{V^{(1)}, V^{(2)}, \ldots, V^{(p)}\}$) is not unique. In this case, although we cannot estimate each vector in $\{V_{\mathcal{N}_i}^{(i)} : i \in F\}$ stably, we can estimate $\sum_{i \in F} V_{\mathcal{N}_i}^{(i)}$ directly and stably using the penalty term $(\min_{i \in F} \tau_i)\|\sum_{i \in F} V_{\mathcal{N}_i}^{(i)}\|_2$. Since $\hat{\beta} = \sum_{i=1}^{p} \hat{V}^{(i)}$, different decompositions of β lead to the same estimation of β.

The predictor duplication method shown above is very convenient to use and has good performance in general. However, when the dimension is high and at the same time the predictor graph is not very sparse, there will be a lot of duplicated predictors in (3) and therefore the predictor duplication method can be inefficient (Obozinski, Jacob, and Vert 2011). In the following Section 3.2, we will propose a new iterative proximal algorithm which does not duplicate predictors. It is stable and very efficient for the high-dimensional data, especially when the predictor graph can be decomposed into several disconnected components.

3.2 Iterative Proximal Algorithm

Given the predictor graph G and positive weights τ_i's, for $\beta \in R^p$, define

$$\|\beta\|_{G,\tau} = \min_{\sum_{i=1}^{p} V^{(i)}=\beta, \ \text{supp}(V^{(i)}) \subseteq \mathcal{N}_i} \sum_{i=1}^{p} \tau_i \|V^{(i)}\|_2. \qquad (4)$$

We can show that $\|\beta\|_{G,\tau}$ is a norm (Obozinski, Jacob, and Vert 2011) and (2) is equivalent to

$$\min_{\beta \in R^p} \frac{1}{2n}\|Y - X\beta\|_2^2 + \lambda \|\beta\|_{G,\tau}. \qquad (5)$$

In problem (5), the squared loss function is strictly convex and differentiable. In addition, $\|\beta\|_{G,\tau}$ is a norm and therefore convex. Thus, we can use the fast iterative shrinkage thresholding algorithm (FISTA) (Beck and Teboulle 2009) to solve it. For our specific problem (5), we propose the following iterative proximal algorithm.

Iterative Proximal (IP) Algorithm

Input: The initial estimate $\beta^{(0)}$ and $L=$ the largest eigenvalue of X^TX/n.
Step 0: Take $Z^{(1)} = \beta^{(0)} \in R^p$ and $t_1 = 1$.

Step m: ($m \geq 1$) Compute

$$h^{(m)} = Z^{(m)} - \frac{1}{nL} X^T (X Z^{(m)} - Y);$$

$$\mathcal{O}^{(m)} = \{i : \|h_{\mathcal{N}_i}^{(m)}\|_2 > \lambda \tau_i / L\};$$

$$\mathcal{S}_{\mathcal{O}^{(m)}} = \{\beta \in R^p : \|\beta_{\mathcal{N}_i}\|_2 \leq \lambda \tau_i / L \text{ for each } i \in \mathcal{O}^{(m)}\};$$

$$\beta^{(m)} = h^{(m)} - \arg\min_{\beta \in \mathcal{S}_{\mathcal{O}^{(m)}}} \|\beta - h^{(m)}\|_2; \qquad (6)$$

$$t_{m+1} = \frac{1 + \sqrt{1 + 4t_m^2}}{2};$$

$$Z^{(m+1)} = \beta^{(m)} + \frac{t_m - 1}{t_{m+1}} (\beta^{(m)} - \beta^{(m-1)}).$$

By Theorem 4.4 in Beck and Teboulle (2009), the sequences $\{\beta^{(m)}\}$ generated via (6) will converge to the optimal solution with rate $O(1/m^2)$. The most time-consuming step in the above IP algorithm is to compute the projection of $h^{(m)}$ onto the convex set $\mathcal{S}_{\mathcal{O}^{(m)}}$. Following the proofs of Lemmas 1 and 2 in Villa et al. (2014), we can show that

$$\beta^{(m)} = h^{(m)} - \arg\min_{\beta \in \mathcal{S}_{\mathcal{O}^{(m)}}} \|\beta - h^{(m)}\|_2$$

$$= \arg\min_\beta \frac{\lambda}{L} \|\beta\|_{G,\tau} + \frac{\|\beta - h^{(m)}\|_2^2}{2}. \qquad (7)$$

Thus, (6) is used to compute the proximal operator of $\frac{\lambda}{L} \|\beta\|_{G,\tau}$ defined as

$$\text{prox}_{\frac{\lambda}{L} \|\beta\|_{G,\tau}} (h^{(m)}) = \arg\min_\beta \frac{\lambda}{L} \|\beta\|_{G,\tau} + \frac{\|\beta - h^{(m)}\|_2^2}{2}. \quad (8)$$

In (6), based on the number of elements in $\mathcal{O}^{(m)}$, denoted as $|\mathcal{O}^{(m)}|$, we use different methods flexibly to find the projection of $h^{(m)}$ onto the convex set $\mathcal{S}_{\mathcal{O}^{(m)}}$ efficiently. If $|\mathcal{O}^{(m)}|$ is small (e.g., smaller than $p/10$ in our simulation study), we calculate the projection by solving the dual problem via the Bertsekas's projected Newton method (Villa et al. 2014). If $|\mathcal{O}^{(m)}|$ is large (e.g., larger than $p/10$), we propose to find the projection by the Parallel Dykstra-like proximal algorithm as shown in Combettes and Pesquet (2011). The details about these two algorithms are shown in the supplementary materials. Furthermore, we note that this IP algorithm is scalable to large-scale problems when the predictor graph G can be decomposed into several components (i.e., the covariance/precision matrix is block diagonal). Denote the disconnected components in G as $G_1, G_2, \ldots, G_K$ with node sets $\mathcal{C}_1, \mathcal{C}_2, \ldots, \mathcal{C}_K$, respectively. In this case, we can compute the proximal operator (8) efficiently by solving the following K subproblems in parallel:

$$\text{prox}_{\frac{\lambda}{L} \|\beta_{\mathcal{C}_k}\|_{G_k, \tau_{\mathcal{C}_k}}} (h_{\mathcal{C}_k}^{(m)}) = \arg\min_{\beta_{\mathcal{C}_k}} \frac{\lambda}{L} \|\beta_{\mathcal{C}_k}\|_{G_k, \tau_{\mathcal{C}_k}} + \frac{\|\beta_{\mathcal{C}_k} - h_{\mathcal{C}_k}^{(m)}\|_2^2}{2},$$

where $\beta_{\mathcal{C}_k}$, $\tau_{\mathcal{C}_k}$, and $h_{\mathcal{C}_k}^{(m)}$ are subvectors of β, τ, and $h^{(m)}$, respectively.

The above parallel computation can potentially save a lot of computational cost. In Section 5.3, we will compare the computational costs of the PD method with our IP algorithm using several simulated examples. In general, the predictor duplication method is very efficient for small datasets. However, when the dimension is high and the predictor graph G is not very sparse, our proposed IP algorithm is much faster than the predictor

duplication method. Furthermore, in some cases, the predictor duplication method may break down since it requires immense working memory.

4. Theoretical Properties

In this section, we study the theoretical properties of our proposed SRIG method. For theoretical study, it is convenient to consider (5) as the objective function. In (5), the optimal decomposition of β minimizing $\|\beta\|_{G,\tau}$ always exists, but may not be unique (Obozinski, Jacob, and Vert 2011). Denote $J_0 = \{i : \beta_i^0 \neq 0\}$, $J_0^c = \{i : \beta_i^0 = 0\}$, and $s_0 = |J_0|$ as the true nonzero coefficient set, the true zero coefficient set, and the number of true nonzero coefficients, respectively. For each $\beta \in R^p$, denote $\mathcal{U}(\beta)$ as the set of all optimal decompositions of β, and $K_{G,\tau}(\beta)$ as the number of nonzero $V^{(i)}$'s in the optimal decomposition of β which has the minimal number of nonzero $V^{(i)}$'s, that is, $K_{G,\tau}(\beta) = \min_{(V^{(1)}, V^{(2)}, \ldots, V^{(p)}) \in \mathcal{U}(\beta)} |\{i : \|V^{(i)}\|_2 \neq 0\}|$. Denote $K_{G,\tau} = \sup_{\text{supp}(\beta) \subseteq J_0} K_{G,\tau}(\beta)$. We can check that $K_{G,\tau} = s_0$ if the graph G has no edge, $K_{G,\tau} = K_0$ if G consists of some disconnected complete subgraphs and J_0 is the union of K_0 node sets of those disconnected subgraphs.

4.1 Subgradient Conditions

The following proposition shows the subgradient conditions for problem (5).

Proposition 1. A vector $\beta \in R^p$ is a solution of (5) if and only if β can be decomposed as $\beta = \sum_{i=1}^p V^{(i)}$ where $V^{(i)}$'s satisfy that, for all $1 \leq i \leq p$, (a) $V_{\mathcal{N}_i^c}^{(i)} = 0$; (b) either $V_{\mathcal{N}_i}^{(i)} \neq 0$ and $X_{\mathcal{N}_i}^T (Y - X\beta) = n\lambda \tau_i \frac{V_{\mathcal{N}_i}^{(i)}}{\|V_{\mathcal{N}_i}^{(i)}\|_2}$, or $V_{\mathcal{N}_i}^{(i)} = 0$ and $\|X_{\mathcal{N}_i}^T (Y - X\beta)\|_2 \leq n\lambda \tau_i$.

The subgradient conditions shown above are similar to the subgradient conditions for the latent group Lasso (Obozinski, Jacob, and Vert 2011) and group Lasso (Nardi and Rinaldo 2008). According to Proposition 1, if $(\hat{V}^{(1)}, \hat{V}^{(2)}, \ldots, \hat{V}^{(p)})$ is a solution of problem (2), then for each i, either $\hat{V}^{(i)} = 0_{p \times 1}$ or $\text{supp}(\hat{V}^{(i)}) = \mathcal{N}_i$. Thus, the estimate $\hat{\beta} = \sum_{i=1}^p \hat{V}^{(i)}$ acquired by our proposed SRIG method has the same decomposition pattern as we discussed in Section 2.

4.2 Connections With Some Existing Methods

The following proposition shows the connections between our proposed SRIG method and several other existing penalized methods when the given predictor graph has some special structures.

Proposition 2. (a) If the predictor graph has no edge, the proposed SRIG method is the same as the adaptive Lasso method for each tuning parameter λ; (b) If the predictor graph consists of K disconnected complete subgraphs, our proposed SRIG method is equivalent to the group Lasso method for each λ; (c) If the predictor graph is a complete graph, our proposed SRIG method has the same nonzero solution set as the ridge regression, that is, for each nonzero solution acquired by ridge regression (or SRIG), SRIG (or ridge regression) could acquire the same solution using a different tuning parameter.

Proposition 2 indicates that the proposed SRIG method includes adaptive Lasso, group Lasso, and ridge regression as special cases. It is much more general and can handle any arbitrary predictor graph structure.

4.3 Finite Sample Bounds

In this section, we derive the oracle inequalities for the prediction and estimation loss of our proposed SRIG method. The design matrix X is treated as fixed in this subsection. For a given graph G, positive weights τ_j's and subset $J \subset \{1, 2 \ldots, p\}$, denote $\mathcal{T}_{G,\tau}(\beta, J)$ as the set of all optimal decompositions of β such that $\sum_{j \in J^c} \tau_j \|V^{(j)}\|_2 \leq 3 \sum_{j \in J} \tau_j \|V^{(j)}\|_2$. For each $1 \leq i \leq p$, denote d_i as the number of predictors in the neighborhood $\mathcal{N}_i$, that is, $d_i = |\mathcal{N}_i|$. The following conditions are considered in this section.

(A1) The errors $\epsilon_1, \epsilon_2, \ldots, \epsilon_n \overset{iid}{\sim} N(0, \sigma^2)$.
(A2) The neighborhood $\mathcal{N}_i \subseteq J_0$ for each $i \in J_0$.
(A3) There exists $\kappa > 0$ such that

$$\inf_{|J| \leq s_0, \beta \in R^p \backslash \{0\}} \quad \inf_{(V^{(1)}, V^{(2)}, \ldots, V^{(p)}) \in \mathcal{T}_{G,\tau}(\beta, J)} \frac{\|X\beta\|_2}{\sqrt{n \sum_{j \in J} \tau_j^2 \|V^{(j)}\|_2^2}}$$

$$\geq \quad \kappa.$$

Note that condition (A1) is a common condition for linear regression. Condition (A2) assumes that the given predictor graph G is "consistent" with β^0, that is, predictors connected to the useful predictor are also useful. Condition (A3) is similar to the restricted eigenvalue conditions used for the group Lasso (Nardi and Rinaldo 2008; Lounici et al. 2011) and the overlapped group Lasso (Percival 2012). It is used to analyze the l_2 consistency property of both estimation and prediction.

Theorem 1. Suppose that conditions (A1), (A2), and (A3) are satisfied. Let $\tau_* = \min_{1 \leq i \leq p} \tau_i$ and denote η_i as the positive square root of the largest eigenvalue of $\frac{1}{n} X_{\mathcal{N}_i}^T X_{\mathcal{N}_i}$. If we choose $\lambda \tau_i \geq \frac{2\sigma \eta_i}{\sqrt{n}} (d_i + A d_i^{1/2} \log(p))^{1/2}$ where $A > 8$, then, for any optimal solution $\hat{\beta}$ of problem (5), we have

$$\frac{1}{n} \|X(\hat{\beta} - \beta^0)\|_2^2 \leq \frac{16\lambda^2 K_{G,\tau}}{\kappa^2}, \quad \|\hat{\beta} - \beta^0\|_{G,\tau}$$

$$\leq \frac{16\lambda K_{G,\tau}}{\kappa^2}, \quad \|\hat{\beta} - \beta^0\|_2 \leq \frac{16\lambda K_{G,\tau}}{\kappa^2 \tau_*},$$

with probability at least $1 - p^{1-q}$, where $q = \frac{1}{8} \min\{A, A^2 \log(p)\}$.

Remark 1. Note that the above results are very general and have close connections with the results shown in the literature. For example, when the predictor graph G has no edge, we have $K_{G,\tau} = s_0$ and $\|\hat{\beta} - \beta^0\|_{G,\tau} = \|\hat{\beta} - \beta^0\|_1$ if $\tau_i = 1$ for each i. Theorem 1 indicates that our proposed SRIG method acquires the same rates of prediction and estimation as the results shown in Bickel, Ritov, and Tsybakov (2009) for the Lasso method. When the given graph G consists of some disconnected complete subgraphs and J_0 is the union of K_0 node sets of those disconnected subgraphs, we have $K_{G,\tau} = K_0$. In this case, we can also recover the results shown in Nardi and Rinaldo (2008) and Lounici et al. (2011) for the group Lasso.

4.4 Asymptotic Normality And Model Selection Consistency

In this section, we first study the asymptotic normality for the case with a fixed dimension p. Then, we study the model selection consistency for the high-dimensional case which allows p to grow with n. Both fixed design and random design are considered in these two cases. For every $\beta \in R^p$, denote β_{J_0} and $\beta_{J_0^c}$ as the subvectors of β with indices in J_0 and J_0^c, respectively.

For the fixed p case, we use the following two common conditions:

(A4) As $n \rightarrow \infty$, $X^T X / n \rightarrow \mathcal{M}$, where $\mathcal{M}$ is a positive matrix.
(A5) The errors $\epsilon_1, \epsilon_2, \ldots, \epsilon_n$ are iid random variables with mean 0 and finite variance σ^2.

Theorem 2. Assume conditions (A2), (A4), and (A5) hold. Suppose the tuning parameter λ and weights τ_i's are chosen such that $\sqrt{n}\lambda \rightarrow 0$ and $n^{(\gamma+1)/2}\lambda \rightarrow \infty$ for some $\gamma > 0$. Furthermore, $\tau_j = O(1)$ for each $j \in J_0$ and $\liminf_{n \rightarrow \infty} n^{-\gamma/2}\tau_j > 0$ for each $j \in J_0^c$. Then, with dimension p fixed, as $n \rightarrow \infty$, we have

$$\sqrt{n}(\hat{\beta}_{J_0} - \beta_{J_0}^0) \xrightarrow{d} N(0, \sigma^2 \mathcal{M}_{J_0,J_0}^{-1}), \text{ and } \hat{\beta}_{J_0^c} \xrightarrow{p} 0,$$

where $\mathcal{M}_{J_0,J_0}$ is the submatrix of $\mathcal{M}$ consisting of the entries with row and column indices in J_0.

Remark 2. Theorem 2 indicates that our proposed SRIG method is estimation-consistent for the fixed p case. It also provides a guideline on how to choose the positive weight τ_j. When $n > p$, similar to the weights used for the Adaptive Lasso (Zou 2006), we can choose $\tau_j = \sqrt{d_j}/|\hat{\beta}_j|^\gamma$, where $\hat{\beta}_j$ is any $\sqrt{n}$-consistent estimate of β_j^0. Note that Theorem 2 can be extended to the random design setting naturally.

Corollary 1. Consider the random design setting where $x_1, x_2, \ldots, x_n$ are iid samples from a multivariate distribution with mean 0 and covariance matrix Σ. Assume that the design matrix X and the errors ϵ are independent. Suppose conditions (A2) and (A5) hold. The tuning parameter λ and weights τ_i's are chosen such that $\sqrt{n}\lambda \rightarrow 0$ and $n^{(\gamma+1)/2}\lambda \rightarrow \infty$ for some $\gamma > 0$. Furthermore, $\tau_j = O(1)$ for each $j \in J_0$ and $\liminf_{n \rightarrow \infty} n^{-\gamma/2}\tau_j > 0$ for each $j \in J_0^c$. Then, with p fixed, as $n \rightarrow \infty$, we have

$$\sqrt{n}(\hat{\beta}_{J_0} - \beta_{J_0}^0) \xrightarrow{d} N(0, \sigma^2 \Sigma_{J_0,J_0}^{-1}), \text{ and } \hat{\beta}_{J_0^c} \xrightarrow{p} 0,$$

where Σ_{J_0,J_0} is the submatrix of Σ consisting of the entries with row and column indices in J_0.

For the high-dimensional case which allows the dimension p to grow with n, if the design matrix X is considered to be fixed, we need the following conditions for model selection consistency:

(A6) The number of nonzero coefficients $s_0 = O(n^{\delta_0})$ for some constant $\delta_0 \in (0, 1)$.
(A7) There exists a constant $Q_1 > 0$ such that $\max_{j \in J_0^c} \|X_j\|_2 \leq \sqrt{n}Q_1$ for each n.
(A8) There exists a constant $Q_2 > 0$ such that the smallest eigenvalue of $X_{J_0}^T X_{J_0}/n$ is larger than Q_2 for each n.
(A9) There exists a constant $\xi \in (0, 1)$ such that $\|X_{J_0^c}^T X_{J_0} (X_{J_0}^T X_{J_0})^{-1}\|_\infty \leq 1 - \xi$, where for a $k \times m$ matrix M, $\|M\|_\infty$ is defined as $\max_{1 \leq i \leq k} \sum_{j=1}^m |M_{ij}|$.

Note that condition (A6) is a common sparsity assumption for the high-dimensional regression problem. Condition (A7) can be satisfied by normalizing each predictor. Condition (A8) guarantees that the matrix $X_{J_0}^T X_{J_0}/n$ is invertible and its inverse behaves well. The main condition (A9) is similar to the strong irrepresentable condition used for Lasso (Zhao and Yu 2006).

Theorem 3. Assume conditions (A1), (A2), and (A6)–(A9) hold. Suppose the weight τ_j is chosen to be $\sqrt{d_j}m_j$ for each j, where the m_j's satisfy that $\max_{j\in J_0} m_j = O_p(1)$ and $\liminf_{n\to\infty} n^{-\gamma} \min_{j\in J_0^c} m_j > 0$ for some $\gamma > \delta_0$. Furthermore, the selected tuning parameter λ and the minimum absolute nonzero coefficient $\beta_{min}^0 = \min_{j\in J_0} |\beta_j^0|$ satisfy that, as $n \longrightarrow \infty$ and $p = p(n) \longrightarrow \infty$,

$$\frac{1}{\lambda}\sqrt{\frac{\log(p-s_0)}{n}} \max_{j\in J_0^c} \frac{\sqrt{d_j}}{\tau_j} \longrightarrow 0, \text{ and } \frac{1}{\beta_{min}^0}(3\sigma\sqrt{\frac{\log s_0}{nQ_2}}$$

$$+\lambda\frac{\sqrt{s_0}}{Q_2}\max_{j\in J_0}\tau_j) \longrightarrow 0.$$

Then, as $n \longrightarrow \infty$ and $p = p(n) \longrightarrow \infty$, there exists a solution $\hat{\beta}$ to (5) such that $\text{sign}(\hat{\beta}) = \text{sign}(\beta^0)$ with probability tending to 1, where $\text{sign}(\cdot)$ maps a positive entry to 1, a negative entry to -1, and zero to zero.

Remark 3. For clarification, we note that many quantities such as p, s_0, λ, τ_j, and d_j depend on n. We use simple notation here for convenience. Theorem 3 indicates that our proposed SRIG method is model-selection-consistent for the high-dimensional case. For example, suppose the dimension $p = O(e^{n^{\delta_1}})$ for some constant $\delta_1 \in (0, 1)$. Furthermore, for sufficiently large n, the minimum absolute nonzero coefficient β_{min}^0 satisfies that $\beta_{min}^0 \geq C_1 n^{(\delta_2-1)/2}$ for some constants $C_1 > 0$ and $\delta_2 > \delta_1$. If we select the weights τ_j's as shown in the theorem and the tuning parameter $\lambda = C_2 n^{(\delta_1-2\delta_0-1)/2}$ for some constant $C_2 > 0$, then by Theorem 3 we can show that there exists a solution $\hat{\beta}$ such that $\text{sign}(\hat{\beta})=\text{sign}(\beta^0)$ with probability tending to 1. In the high-dimensional case with $p \gg n$, our simulation study suggests that choosing $\tau_j = \sqrt{d_j}/|\hat{cov}(X_j, Y)|^\gamma$ works well. The positive parameter γ can be chosen by cross-validation.

In Theorem 3, as the Lasso method, we use the irrepresentable condition (A9). In fact, we can also use the following condition (A9′) to reflect the use of the weights τ_j's. Following the same proof of Theorem 3, we can achieve the model selection consistency as shown in Corollary 2.

(A9′) There exists a constant $\xi \in (0, 1)$ such that for each $j \in J_0^c$, we have

$$\|X_{\mathcal{N}_j}^T X_{J_0}(X_{J_0}^T X_{J_0})^{-1}\|_\infty \leq \frac{\tau_j}{\sqrt{d_j}}(1-\xi).$$

Corollary 2. Assume conditions (A1), (A2), (A6)–(A8), and (A9′) hold. Suppose the weight τ_j's satisfy that $\sqrt{s_0}\max_{j\in J_0}\tau_j = o_p(1)$. Furthermore, the selected tuning parameter λ and the minimum absolute nonzero coefficient $\beta_{min}^0 = \min_{j\in J_0}|\beta_j^0|$ satisfy the same conditions in Theorem 3, then, as $n \longrightarrow \infty$ and $p = p(n) \longrightarrow \infty$, there exists a solution $\hat{\beta}$ to (5) such that $\text{sign}(\hat{\beta}) = \text{sign}(\beta^0)$ with probability tending to 1.

Theorem 3 considers the fixed design setting. It can be extended to the random design setting as well. For that setting, the conditions (A6)–(A9) are replaced by the following conditions:

(A10) Let $x_1, x_2, \ldots, x_n \overset{iid}{\sim} N(0, \Sigma)$ with $\Sigma_{jj} = 1$ for each j. Furthermore, assume that X and ϵ are independent. The dimension $p < e^{n/4Q_3^2}$, where $Q_3 > 4\sqrt{5/3}$.

(A11) Restricted eigenvalue assumption:

$$\Lambda_{\min}(s_0) = \frac{16}{17} \min_{J\subseteq\{1,2,\ldots,p\},\ |J|\leq s_0}\ \min_{\theta\neq 0,\ \theta_{J^c}=0} \frac{\theta^T\Sigma\theta}{\|\theta_J\|_2^2} > 0.$$

(A12) The number of true nonzero coefficients $s_0 < (\Lambda_{min}(s_0)/16Q_3)\sqrt{n/\log p}$.

Note that conditions (A10)–(A12) are common conditions used in the literature for the random design setting (Bickel, Ritov, and Tsybakov 2009; Zhou, van de Geer, and Bühlmann 2009). Under these conditions, we can show that our proposed SRIG method is also model-selection-consistent for the high-dimensional case with random design.

Theorem 4. Assume conditions (A1), (A2), and (A10)–(A12) hold. Suppose the weight τ_j is chosen to be $\sqrt{d_j}m_j$ for each j, where $s_0^{3/2}\max_{j\in J_0} m_j = o(\sqrt{\Lambda_{\min}(s_0)}\min_{j\in J_0^c} m_j)$. Furthermore, the selected tuning parameter λ and the minimum absolute nonzero coefficient $\beta_{\min}^0 = \min_{j\in J_0} |\beta_j^0|$ satisfy that, as $n \longrightarrow \infty$ and $p = p(n) \longrightarrow \infty$,

$$\frac{1}{\lambda}\sqrt{\frac{\log(p-s_0)}{n}} \max_{j\in J_0^c} \frac{\sqrt{d_j}}{\tau_j} \longrightarrow 0,$$

$$\frac{1}{\beta_{\min}^0}\left(3\sigma\sqrt{\frac{\log s_0}{n\Lambda_{\min}(s_0)}} + \lambda\frac{\sqrt{s_0}}{\Lambda_{\min}(s_0)}\max_{j\in J_0}\tau_j\right) \longrightarrow 0.$$

Then, as $n \longrightarrow \infty$ and $p = p(n) \longrightarrow \infty$, there exists a solution $\hat{\beta}$ to (5) such that $\text{sign}(\hat{\beta}) = \text{sign}(\beta^0)$ with probability tending to 1, where $\text{sign}(\cdot)$ maps a positive entry to 1, a negative entry to -1, and zero to zero.

Remark 4. Under conditions (A10)–(A12), we can show that condition (A7) is satisfied with $Q_1 = \sqrt{3/2}$, condition (A8) is satisfied with $Q_2 = \Lambda_{min}(s_0)$, and $\|X_{J_0^c}^T X_{J_0}(X_{J_0}^T X_{J_0})^{-1}\|_\infty \leq \sqrt{3s_0/(2\Lambda_{min}(s_0))}$, with probability greater than $1 - 1/p^2$. Based on these results, we can use a similar proof of Theorem 3 to prove Theorem 4.

5. Simulation Study

In this section, we first compare our proposed SRIG method with many existing methods. Then, we conduct a sensitivity study of the SRIG method. Finally, we compare the computational costs of the predictor duplication method and our proposed iterative proximal algorithm using some simulated examples.

5.1 Performance Comparison

To examine the performance of SRIG, we compare it with many other methods on three examples. First, we compare SRIG

with popular penalized methods such as Lasso, ridge regression, adaptive lasso (ALasso), and elastic net (Enet) which do not use the predictor graph structure information directly. Second, we compare SRIG with some existing methods using the predictor structure information. The competitors are GRACE (Li and Li 2008) and GOSCAR (Yang et al. 2012). Third, we compare SRIG with other latent component approaches such as principal component regression (PCR) and sparse partial least squares (SPLS) using the R packages *pls* (Mevik and Wehrens 2007) and *spls* (Chung, Chun, and Keles 2012), respectively. In this simulation study, the predictor graph is defined by the precision matrix of the predictors. The performance of GRACE, GOSCAR, and SRIG using both the estimated predictor graph and the oracle true predictor graph are evaluated on all examples. We denote GRACE-O, GOSCAR-O, and SRIG-O as the GRACE, GOSCAR, and SRIG methods using the true predictor graph, respectively. For comparison, we also show the performance of the least square method based on the true model, which is denoted as LS-O.

We generate data from model (1) with the errors $\epsilon_1, \epsilon_2, \ldots, \epsilon_n \overset{iid}{\sim} N(0, \sigma^2)$. For each example, our simulated data include a training set, an independent validation set, and an independent test set. All the models are fitted on the training data only. The validation data are used to choose the tuning parameter and the test dataset is used to evaluate different methods. We use the notation ./././ to show the sample sizes in the training, validation, and test sets, respectively. For each example, we consider three cases: (I) 40/40/400, (II) 80/80/400, and (III) 120/120/400. For each case, we repeat the simulation 50 times. The predictor graph is estimated by the graphical Lasso method (Friedman, Hastie, and Tibshirani 2008) only using the training data in all cases.

Example 1: (Ω is block diagonal). $p = 100$, $s_0 = 15$, $\sigma = 5$, and the true coefficient vector $\beta^0 = (3, 3, \ldots, 3, 0, 0, \ldots, 0)^T$. The predictors are generated as:

$$X_j = Z_1 + 0.4\epsilon_j^x, \ \ Z_1 \sim N(0, 1), \ \ 1 \leq j \leq 5;$$
$$X_j = Z_2 + 0.4\epsilon_j^x, \ \ Z_2 \sim N(0, 1), \ \ 6 \leq j \leq 10,$$
$$X_j = Z_3 + 0.4\epsilon_j^x, \ \ Z_3 \sim N(0, 1), \ \ 11 \leq j \leq 15; \ \ X_j \overset{i.i.d}{\sim} N(0, 1), \ \ 16 \leq j \leq 100,$$

where $\epsilon_j^x \overset{iid}{\sim} N(0, 1)$, $j = 1, 2, \ldots, 15$.

Example 2: (Ω is banded). $p = 100$, $\sigma = 10$, and β^0 is the same as the β^0 used in Example 1. The predictors $(X_1, X_2, \ldots, X_p)^T \sim N(0, \Sigma)$ with $\Sigma_{ij} = 0.5^{|i-j|}$. For this example, we have $\omega_{ii} = 1.333$, $\omega_{ij} = -0.667$ if $|i - j| = 1$ and $\omega_{ij} = 0$ if $|i - j| > 1$.

Example 3: (Ω is sparse). $p = 100$, $\sigma = 5$, and the predictors $(X_1, X_2, \ldots, X_p)^T \sim N(0, \Omega^{-1})$, where $\Omega = B + \delta I$. Each off-diagonal entry in B is generated independently and equals to 0.5 with probability 0.05, or 0 with probability 0.95. The diagonal entry of B is 0. Here, δ is chosen such that the conditional number of Ω is equal to p. Finally, Ω is standardized to have unit diagonals. We set $\beta^0 = \Omega\Sigma_{xy}$, where
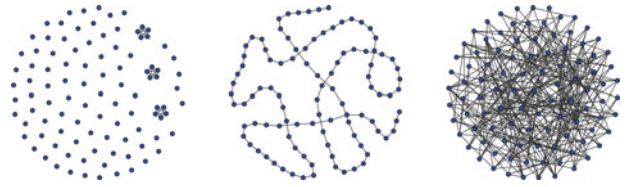

Figure 1. True predictor graphs of three simulation examples.

$\Sigma_{xy} = (c_1, c_2, \ldots, c_p)^T$ with $c_i = 10$ for the predictors having the top four largest degrees and $c_i = 0$ otherwise.

To evaluate different methods, we use the following measures:
- l_2 distance $\|\hat{\beta} - \beta^0\|_2$;
- Relative prediction error (RPE) $\frac{1}{\sigma^2 N_{\text{test}}}(\hat{\beta} - \beta^0)^T X_{\text{test}}^T X_{\text{test}}(\hat{\beta} - \beta^0)$, where X_{test} is the test samples and N_{test} is the number of test samples;
- False positive rate (FPR) and false negative rate (FNR);
- Nonzero match ratio (NMR) $= \frac{|\{(i,j): \ \Omega_{ij} \neq 0, \ \hat{\beta}_i \neq 0, \ \hat{\beta}_j \neq 0\}|}{|\{(i,j): \ \Omega_{ij} \neq 0, \ \beta_i^0 \neq 0, \ \beta_j^0 \neq 0\}|}$, which is used to check whether the estimated coefficients of two connected useful predictors are both nonzero; Zero match ratio (ZMR) $= \frac{|\{(i,j): \ \Omega_{ij} \neq 0, \ \hat{\beta}_i = 0, \ \hat{\beta}_j = 0\}|}{|\{(i,j): \ \Omega_{ij} \neq 0, \ \beta_i^0 = 0, \ \beta_j^0 = 0\}|}$, which is used to check whether the estimated coefficients of two connected useless predictors are both zero. We use NMR and ZMR when there is at least one edge connecting two useful predictors and one edge connecting two useless predictors. Thus, these two ratios are well defined and always between 0 and 1.

Figure 1 shows the true predictor graphs (defined by Ω) of these three examples. The numbers of edges for these three graphs are 30, 99, and 243, respectively. Such graphs were also studied in the literature previously (Yang et al. 2012; Cai, Liu, and Luo 2011). It is very interesting to study whether the structure information represented by these predictor graphs could be used to improve the performance of estimation, prediction, and model selection. Tables 1– 2 show the performance comparison for Example 1. The comparison results indicate that the Elastic net method acquires better estimation and prediction than Lasso, ridge regression and adaptive Lasso methods by using a linear combination of l_1 and ridge penalty. The GOSCAR and GRACE methods further improve the performance of estimation and prediction benefiting from using the addtional estimated predictor graph directly. However, Elastic net, GOSCAR, and GRACE methods still have relatively high FPR. Compared with the other methods (not including methods using the true predictor graph), our proposed SRIG method delivers the best performance of estimation and prediction. Furthermore, SRIG almost always identifies the true model perfectly for this example. Since the estimated predictor graph for this example is almost the same as the true predictor graph, the performance of GOSCAR-O, GRACE-O, and SRIG-O are similar to those of GOSCAR, GRACE, and SRIG, respectively. Due to the strong correlation between different important predictors, the performance of LS-O method on this example is not very good. Compared with LS-O, our SRIG method still acquires competitive performance.

Table 1. Performance comparison of estimation and prediction for Example 1.

Methods	l_2 distance			RPE		
	(I)	(II)	(III)	(I)	(II)	(III)
LS-O	8.378 (0.323)	5.014 (0.124)	4.132 (0.142)	0.595 (0.047)	0.212 (0.010)	0.149 (0.010)
Lasso	8.527 (0.199)	5.635 (0.119)	4.328 (0.153)	1.291 (0.087)	0.530 (0.036)	0.274 (0.014)
Ridge	8.166 (0.050)	7.585 (0.039)	4.325 (0.062)	12.336 (0.215)	10.936 (0.144)	0.946 (0.027)
ALasso	8.822 (0.275)	5.570 (0.167)	4.686 (0.147)	1.032 (0.093)	0.351 (0.041)	0.211 (0.012)
Enet	5.120 (0.201)	3.770 (0.110)	3.265 (0.092)	0.969 (0.071)	0.431 (0.031)	0.239 (0.012)
PCR	7.097 (0.104)	5.730 (0.096)	4.846 (0.080)	5.256 (0.253)	2.714 (0.134)	1.670 (0.092)
SPLS	4.147 (0.307)	3.150 (0.234)	2.752 (0.187)	1.046 (0.141)	0.777 (0.105)	0.494 (0.049)
GOSCAR	4.980 (0.273)	3.218 (0.139)	3.038 (0.108)	0.817 (0.070)	0.362 (0.024)	0.252 (0.010)
GOSCAR-O	5.051 (0.270)	3.220 (0.138)	3.027 (0.107)	0.811 (0.069)	0.363 (0.024)	0.255 (0.010)
GRACE	4.551 (0.142)	3.749 (0.091)	3.378 (0.122)	0.632 (0.050)	0.338 (0.021)	0.222 (0.011)
GRACE-O	4.554 (0.140)	3.743 (0.091)	3.371 (0.123)	0.633 (0.051)	0.338 (0.021)	0.222 (0.011)
SRIG	2.403 (0.065)	1.890 (0.064)	1.610 (0.046)	0.324 (0.037)	0.217 (0.015)	0.175 (0.013)
SRIG-O	2.392 (0.065)	1.820 (0.045)	1.564 (0.043)	0.320 (0.037)	0.208 (0.015)	0.171 (0.012)

Table 2. Performance comparison of model selection for Example 1.

Methods	FPR			FNR		
	(I)	(II)	(III)	(I)	(II)	(III)
LS-O	0.000 (0.000)	0.000 (0.000)	0.000 (0.000)	0.000 (0.000)	0.000 (0.000)	0.000 (0.000)
Lasso	0.087 (0.009)	0.145 (0.014)	0.123 (0.010)	0.171 (0.012)	0.027 (0.005)	0.003 (0.002)
Ridge	1.000 (0.000)	1.000 (0.000)	1.000 (0.000)	0.000 (0.000)	0.000 (0.000)	0.000 (0.000)
ALasso	0.039 (0.007)	0.027 (0.006)	0.041 (0.005)	0.173 (0.016)	0.021 (0.006)	0.007 (0.003)
Enet	0.131 (0.013)	0.171 (0.012)	0.148 (0.013)	0.032 (0.010)	0.000 (0.000)	0.000 (0.000)
PCR	1.000 (0.000)	1.000 (0.000)	1.000 (0.000)	0.000 (0.000)	0.000 (0.000)	0.000 (0.000)
SPLS	0.140 (0.034)	0.274 (0.043)	0.245 (0.034)	0.043 (0.011)	0.004 (0.002)	0.003 (0.002)
GOSCAR	0.190 (0.025)	0.226 (0.007)	0.307 (0.009)	0.039 (0.011)	0.003 (0.002)	0.000 (0.000)
GOSCAR-O	0.230 (0.032)	0.228 (0.007)	0.310 (0.009)	0.036 (0.011)	0.003 (0.002)	0.000 (0.000)
GRACE	0.136 (0.011)	0.135 (0.009)	0.127 (0.011)	0.005 (0.004)	0.000 (0.000)	0.000 (0.000)
GRACE-O	0.138 (0.011)	0.134 (0.009)	0.127 (0.011)	0.005 (0.004)	0.000 (0.000)	0.000 (0.000)
SRIG	0.001 (0.001)	0.003 (0.001)	0.003 (0.001)	0.000 (0.000)	0.000 (0.000)	0.000 (0.000)
SRIG-O	0.000 (0.000)	0.000 (0.000)	0.000 (0.000)	0.000 (0.000)	0.000 (0.000)	0.000 (0.000)

Table 3. Performance comparison of estimation and prediction for Example 2.

Methods	l_2 distance			RPE		
	(I)	(II)	(III)	(I)	(II)	(III)
LS-O	9.312 (0.322)	6.193 (0.213)	4.926 (0.146)	0.575 (0.036)	0.235 (0.015)	0.149 (0.008)
Lasso	9.896 (0.205)	7.440 (0.159)	5.865 (0.130)	1.146 (0.061)	0.536 (0.022)	0.300 (0.012)
Ridge	9.298 (0.065)	8.571 (0.049)	6.496 (0.079)	2.240 (0.045)	1.914 (0.028)	0.500 (0.015)
ALasso	10.072 (0.192)	7.311 (0.181)	6.238 (0.157)	1.065 (0.056)	0.426 (0.021)	0.275 (0.011)
Enet	8.776 (0.197)	6.668 (0.142)	5.176 (0.103)	1.056 (0.057)	0.514 (0.023)	0.280 (0.011)
PCR	9.782 (0.110)	8.842 (0.125)	8.613 (0.132)	2.318 (0.071)	1.763 (0.074)	1.711 (0.077)
SPLS	8.423 (0.261)	5.480 (0.212)	4.062 (0.172)	0.900 (0.056)	0.321 (0.024)	0.194 (0.017)
GOSCAR	8.844 (0.243)	6.280 (0.173)	4.547 (0.123)	0.974 (0.051)	0.438 (0.023)	0.221 (0.009)
GOSCAR-O	5.662 (0.247)	4.666 (0.121)	4.416 (0.102)	0.566 (0.049)	0.287 (0.016)	0.208 (0.010)
GRACE	8.815 (0.235)	6.562 (0.152)	5.270 (0.112)	1.029 (0.055)	0.475 (0.021)	0.267 (0.011)
GRACE-O	8.238 (0.239)	6.353 (0.151)	5.084 (0.108)	0.972 (0.062)	0.453 (0.022)	0.254 (0.010)
SRIG	8.179 (0.200)	5.890 (0.130)	4.942 (0.104)	0.949 (0.068)	0.396 (0.022)	0.236 (0.009)
SRIG-O	7.354 (0.193)	5.257 (0.133)	4.245 (0.097)	0.718 (0.050)	0.284 (0.016)	0.167 (0.008)

Tables 3–4 display the results for Example 2. As Example 1, the Elastic net method has better performance of estimation and prediction than Lasso and ridge regression. For the cases with relative large sample sizes, the adaptive Lasso method acquires better prediction than the Elastic net method. GOSCAR, GRACE, and our proposed SRIG obtain better estimation and prediction than the methods not incorporating the additional predictor graph information. Methods using the true predictor graph acquire better estimation and prediction than those methods using estimated predictor graph, especially for the small sample cases (I and II). Compared with GOSCAR (GOSCAR-O) and GRACE (GRACE-O), our proposed SRIG (SRIG-O) has competitive performance of estimation and prediction. Furthermore, the results in Table 4 show that our proposed SRIG-O method acquires much lower FPR than the GOSCAR-O and GRACE-O methods. This indicates that GRACE and GOSCAR methods using the predictor graph edge-by-edge may lead to poor model selection results, although they can acquire competitive performance for estimation and prediction. Compared with latent component approaches, SRIG has better performance than PCR while worse performance than SPLS. However, SRIG-O has better performance than PCR and SPLS in most cases.

Table 4. Performance comparison of model selection for Example 2.

Methods	FPR			FNR		
	(I)	(II)	(III)	(I)	(II)	(III)
LS-O	0.000 (0.000)	0.000 (0.000)	0.000 (0.000)	0.000 (0.000)	0.000 (0.000)	0.000 (0.000)
Lasso	0.154 (0.010)	0.171 (0.014)	0.158 (0.011)	0.304 (0.016)	0.099 (0.010)	0.025 (0.005)
Ridge	1.000 (0.000)	1.000 (0.000)	1.000 (0.000)	0.000 (0.000)	0.000 (0.000)	0.000 (0.000)
ALasso	0.121 (0.012)	0.071 (0.010)	0.081 (0.007)	0.303 (0.018)	0.121 (0.014)	0.052 (0.009)
Enet	0.311 (0.032)	0.273 (0.024)	0.223 (0.016)	0.168 (0.019)	0.051 (0.009)	0.005 (0.003)
PCR	1.000 (0.000)	1.000 (0.000)	1.000 (0.000)	0.000 (0.000)	0.000 (0.000)	0.000 (0.000)
SPLS	0.196 (0.030)	0.050 (0.011)	0.059 (0.021)	0.181 (0.021)	0.096 (0.013)	0.043 (0.007)
GOSCAR	0.271 (0.028)	0.369 (0.030)	0.354 (0.026)	0.164 (0.016)	0.027 (0.007)	0.005 (0.003)
GOSCAR-O	0.500 (0.038)	0.569 (0.020)	0.715 (0.017)	0.023 (0.008)	0.003 (0.002)	0.000 (0.000)
GRACE	0.440 (0.055)	0.203 (0.014)	0.174 (0.011)	0.109 (0.017)	0.055 (0.008)	0.011 (0.003)
GRACE-O	0.328 (0.045)	0.195 (0.013)	0.170 (0.011)	0.113 (0.016)	0.047 (0.008)	0.009 (0.003)
SRIG	0.283 (0.016)	0.275 (0.017)	0.243 (0.014)	0.112 (0.014)	0.028 (0.005)	0.009 (0.004)
SRIG-O	0.170 (0.016)	0.101 (0.013)	0.067 (0.008)	0.099 (0.012)	0.033 (0.006)	0.013 (0.004)

Table 5. Performance comparison of estimation and prediction for Example 3.

Methods	l_2 distance			RPE		
	(I)	(II)	(III)	(I)	(II)	(III)
LS-O	2.668 (0.103)	1.769 (0.055)	1.324 (0.048)	0.401 (0.027)	0.172 (0.010)	0.103 (0.007)
Lasso	11.370 (0.131)	7.096 (0.186)	4.772 (0.106)	3.792 (0.080)	1.850 (0.090)	0.846 (0.035)
Ridge	12.140 (0.008)	12.100 (0.013)	11.026 (0.166)	4.006 (0.035)	3.979 (0.046)	3.779 (0.059)
ALasso	11.339 (0.147)	7.070 (0.184)	4.773 (0.105)	3.786 (0.078)	1.840 (0.088)	0.843 (0.035)
Enet	11.366 (0.129)	7.096 (0.186)	4.772 (0.106)	3.795 (0.076)	1.850 (0.090)	0.846 (0.035)
PCR	12.122 (0.010)	12.140 (0.007)	12.139 (0.008)	4.216 (0.044)	4.072 (0.043)	4.076 (0.049)
SPLS	12.080 (0.124)	11.219 (0.137)	10.858 (0.111)	5.990 (0.165)	5.247 (0.112)	4.664 (0.115)
GOSCAR	8.879 (0.220)	5.677 (0.151)	4.001 (0.090)	2.671 (0.117)	1.175 (0.056)	0.600 (0.025)
GOSCAR-O	8.709 (0.220)	5.454 (0.142)	3.900 (0.085)	2.510 (0.102)	1.094 (0.052)	0.571 (0.023)
GRACE	11.166 (0.140)	7.074 (0.184)	4.788 (0.105)	3.753 (0.088)	1.842 (0.089)	0.850 (0.035)
GRACE-O	10.140 (0.159)	7.085 (0.186)	4.787 (0.104)	3.279 (0.071)	1.822 (0.086)	0.848 (0.035)
SRIG	6.398 (0.223)	3.756 (0.131)	2.691 (0.076)	1.607 (0.093)	0.621 (0.040)	0.322 (0.018)
SRIG-O	4.150 (0.301)	2.344 (0.098)	1.736 (0.066)	0.804 (0.103)	0.254 (0.020)	0.141 (0.009)

Table 6. Performance comparison of model selection for Example 3.

Methods	FPR			FNR		
	(I)	(II)	(III)	(I)	(II)	(III)
LS-O	0.000 (0.000)	0.000 (0.000)	0.000 (0.000)	0.000 (0.000)	0.000 (0.000)	0.000 (0.000)
Lasso	0.152 (0.019)	0.467 (0.015)	0.481 (0.013)	0.793 (0.027)	0.129 (0.018)	0.011 (0.005)
Ridge	1.000 (0.000)	1.000 (0.000)	1.000 (0.000)	0.000 (0.000)	0.000 (0.000)	0.000 (0.000)
ALasso	0.155 (0.020)	0.469 (0.014)	0.473 (0.014)	0.776 (0.031)	0.124 (0.017)	0.011 (0.005)
Enet	0.233 (0.031)	0.467 (0.015)	0.481 (0.013)	0.716 (0.034)	0.129 (0.018)	0.011 (0.005)
PCR	1.000 (0.000)	1.000 (0.000)	1.000 (0.000)	0.000 (0.000)	0.000 (0.000)	0.000 (0.000)
SPLS	0.440 (0.050)	0.351 (0.044)	0.305 (0.042)	0.502 (0.053)	0.493 (0.046)	0.476 (0.049)
GOSCAR	0.292 (0.028)	0.378 (0.022)	0.380 (0.011)	0.438 (0.031)	0.060 (0.010)	0.004 (0.003)
GOSCAR-O	0.261 (0.024)	0.349 (0.016)	0.369 (0.012)	0.424 (0.030)	0.049 (0.009)	0.004 (0.003)
GRACE	0.220 (0.030)	0.472 (0.015)	0.481 (0.014)	0.711 (0.036)	0.120 (0.018)	0.011 (0.005)
GRACE-O	0.677 (0.058)	0.531 (0.028)	0.480 (0.014)	0.296 (0.055)	0.085 (0.015)	0.009 (0.004)
SRIG	0.216 (0.012)	0.266 (0.017)	0.245 (0.016)	0.109 (0.014)	0.015 (0.005)	0.000 (0.000)
SRIG-O	0.163 (0.018)	0.127 (0.018)	0.071 (0.015)	0.031 (0.018)	0.000 (0.000)	0.000 (0.000)

The performance comparison for Example 3 is shown in Tables 5 and 6. Methods not using the predictor graph have poor performance for estimation, prediction, and model selection, especially for the cases (I) and (II) with smaller n than p. For this example, the performance of estimation and prediction of the Elastic net method is similar to Lasso, ridge regression, and adaptive Lasso. When the additional predictor graph information is used, the GRACE method, which can be considered as a graph version of the Elastic net, still does not acquire improved performance. However, GOSCAR benefits from the additional predictor graph information and acquires better performance. Compared with the other methods (not including SRIG-O), our

proposed SRIG method has the best results for estimation, prediction, and model selection. As the previous two examples, each method using the true predictor graph performs better than the corresponding method using the estimated graph. For this example, LS-O acquires the best performance and our proposed SRIG-O method has similar results to the LS-O method when the sample size is large.

The comparison results of NMR and ZMR for the cases with sample sizes 40/40/400 are shown in Table 7. The results for the cases with samples sizes 80/80/400 and 120/120/400 are shown in the supplementary materials. Compared with the other methods (except LS-O which uses the underlying true model), our

Table 7. Performance comparison of NMR and ZMR (Sample sizes: 40/40/400).

Methods	NMR			ZMR		
	Example 1	Example 2	Example 3	Example 1	Example 2	Example 3
LS-O	1.000 (0.000)	1.000 (0.000)	1.000 (0.000)	–	1.000 (0.000)	1.000 (0.000)
Lasso	0.679 (0.020)	0.480 (0.025)	0.149 (0.025)	–	0.717 (0.017)	0.743 (0.031)
Ridge	1.000 (0.000)	1.000 (0.000)	1.000 (0.000)	–	0.000 (0.000)	0.000 (0.000)
Alasso	0.681 (0.027)	0.494 (0.026)	0.167 (0.029)	–	0.779 (0.021)	0.738 (0.032)
Enet	0.939 (0.019)	0.710 (0.032)	0.215 (0.034)	–	0.520 (0.038)	0.642 (0.037)
PCR	1.000 (0.000)	1.000 (0.000)	1.000 (0.000)	–	0.000 (0.000)	0.000 (0.000)
SPLS	0.922 (0.020)	0.703 (0.033)	0.445 (0.057)	–	0.702 (0.038)	0.441 (0.056)
GOSCAR	0.927 (0.019)	0.717 (0.026)	0.491 (0.032)	–	0.593 (0.032)	0.528 (0.029)
GOSCAR-O	0.933 (0.019)	0.966 (0.012)	0.505 (0.032)	–	0.405 (0.040)	0.574 (0.028)
GRACE	0.989 (0.008)	0.813 (0.029)	0.227 (0.036)	–	0.462 (0.048)	0.658 (0.037)
GRACE-O	0.989 (0.008)	0.809 (0.027)	0.676 (0.059)	–	0.552 (0.040)	0.271 (0.052)
SRIG	1.000 (0.000)	0.841 (0.019)	0.864 (0.018)	–	0.579 (0.020)	0.627 (0.018)
SRIG-O	1.000 (0.000)	0.844 (0.017)	0.969 (0.018)	–	0.780 (0.020)	0.713 (0.030)

Note: [– indicates that value is not available since there are no edges between useless predictors.]

proposed SRIG-O acquires the best performance in most cases. The NMR's of SRIG-O indicate that our proposed SRIG method incorporates most edges between useful predictors efficiently and therefore chooses those connected useful predictors simultaneously. The ZMR's of SRIG-O indicate that our proposed SRIG-O method also makes use of most edges between useless predictors and therefore excludes those connected useless predictors jointly. Overall, for our proposed SRIG method, the estimated pattern (zero or nonzero) among coefficients agrees with the graphical structure very well.

In conclusion, the simulation results indicate that our proposed SRIG method can make use of the structure information among predictors efficiently and performs well forestimation, prediction, and model selection.

5.2 Sensitivity Study

An important condition for our proposed SRIG method is the condition (A2) which requires that the predictor graph G is "consistent" with the true coefficients vector β^0, that is, predictors connected to the useful predictor are also useful. Since it is difficult to check this condition in practice, it is very important to study the performance of SRIG when the condition (A2) is violated.

To this end, we evaluate the performance of SRIG on a series of datasets with changing predictor graphs. Fix $p = 100$, $\sigma = 3$, $s_0 = 20$, and $\beta^0 = (20, 2, 2, \ldots, 2, 0, 0, \ldots, 0)^T$. For each $p^* = 0, 1, \ldots, 30$, we generate the predictor matrix X from $N(0, \Omega^{-1})$, where $\Omega = B + 2|\lambda_{\max}(B)|I_p$. Here, $B_{ii} = 2$ for each $1 \leq i \leq p$, $B_{1i} = B_{i1} = 0.3$ for each $1 \leq i \leq (s_0 + p^*)$, $B_{(s_0+1)i} = B_{i(s_0+1)} = 0.3$ for each $(s_0 + 1) \leq i \leq p$, and $B_{ij} = 0$ otherwise. $\lambda_{\max}(B)$ is the largest eigenvalue of the matrix B. Finally, Ω is standardized to have unit diagonals.

For this study, the true precision matrix Ω is used to construct the predictor graph G. The neighborhoods of the useful predictor X_1 and the useless predictor X_{s_0+1} are $\mathcal{N}_1 = \{1, 2, \ldots, s_0 + p^*\}$ and $\mathcal{N}_{s_0+1} = \{s_0 + 1, s_0 + 2, \ldots, p\}$, respectively. The number of predictors shared by these two neighborhood is $|\mathcal{N}_1 \cap \mathcal{N}_{s_0+1}| = |\{s_0 + 1, s_0 + 2, \ldots, s_0 + p^*\}| = p^*$. The condition (A2) is satisfied when $p^* = 0$ and will be violated more and more seriously as p^* increases. Based on this example, we study the robustness of SRIG as p^* changes gradually from 0

to 30. For each p^*, we also evaluate the performance of Lasso method. The sample sizes are fixed as 80/80/400.

Figure 2 shows the performances of SRIG and Lasso method as the number of shared predictors p^* increases. It indicates that Lasso method is more robust than our proposed SRIG method to the intersection between the neighborhood of useful predictors and the neighborhood of useless predictors. One possible reason is that Lasso does not use the predictor graph information directly. For our proposed SRIG method, as p^* increases, the condition (A2) is more and more violated and the performance of SRIG gets worse. As shown in Figure 2, if the condition (A2) is not violated seriously, our proposed SRIG method still has better performance than the Lasso method. However, if (A2) is violated seriously (i.e., $p^* > 25$), the Lasso method performs better than our proposed SRIG method. Besides this study, we also compare SRIG with the other methods on an additional example where the positions of useful predictors in Example 2 are adjusted so that the condition (A2) is much violated. The simulation results (shown in the supplementary materials) indicate that our proposed SRIG method still performs as well as the other methods.

5.3 PD Method vs IP Algorithm

In this subsection, we compare the computational costs of the PD method and our proposed IP algorithm by some examples. Besides the Examples 1–3 shown in Section 5.1, we also consider the following three high-dimensional examples:

Example 4: $n = 400$, $p = 1500$, $s_0 = 25$, $\sigma = 5$, and the true coefficient vector $\beta^0 = (1, 1, \ldots, 1, 0, \ldots, 0)^T$. The predictors are generated as follows.

$$X_j = Z_1 + \epsilon_j^x, \ \ Z_1 \sim N(0, 1), \ \ 1 \leq j \leq 25,$$
$$X_j = Z_2 + \epsilon_j^x, \ \ Z_2 \sim N(0, 1), \ \ 26 \leq j \leq 50,$$
$$(X_{51}, X_{52}, \ldots, X_p)^T \sim N(0, \Omega_*^{-1}),$$

where $\epsilon_j^x \overset{iid}{\sim} N(0, 1)$, $j = 1, 2, \ldots, 50$ and $\Omega_* = B + \delta I$. Each off-diagonal entry in B is generated independently and equals to 0.5 with probability 0.25, or 0 with probability 0.75. The diagonal entry of B is 0. Here, δ is chosen such that the conditional number of Ω_* is equal to $p - 50$. Finally, Ω_* is standardized to have unit diagonals.
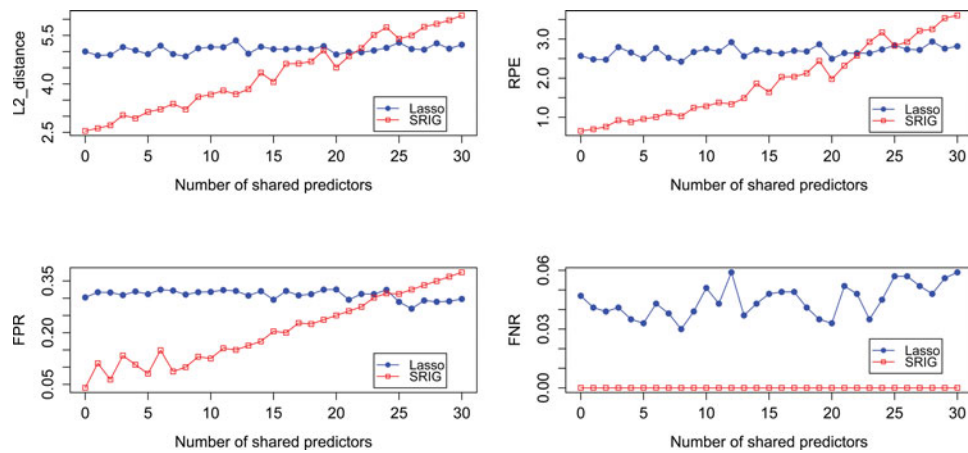
Figure 2. Sensitivity study of the SRIG method.

Example 5: $n = 500$, $p = 2000$ and the other setup is the same as Example 4.

Example 6: $n = 600$, $p = 2500$ and the other setup is the same as Example 4.

For these six examples, we use both the PD method (using `gglasso` R package) and our proposed IP algorithm to compute the solution path of the SRIG method using the true predictor graph. To be specific, we set all the weights τ_i's to be 1 and compute the set of solutions corresponding to 100 different values of the tuning parameter $\lambda_1 > \lambda_2 > \ldots > \lambda_{100}$, where $\lambda_1 = \|X^T Y / n\|_2$ which shrinks all the parameters to be 0 and $\lambda_{100} = 0.05\lambda_1$. The computational times (in seconds) of PD method and IP algorithm are shown in Table 8.

As shown in Table 8, both methods require more time to compute the solution path as the dimension p and the number of edges in the predictor graph increase. When p is small and at the same time the predictor graph G is sparse (e.g., Examples 1–3), the PD method is faster than the IP algorithm. However, for high-dimensional datasets with complicated predictor graphs (e.g., Examples 4–6), our proposed IP algorithm is more efficient than the PD method. For Example 6, the PD method using `gglasso` package breaks down due to out of memory while our proposed IP algorithm still works well. In this case, the proposed IP algorithm is very desirable.

6. Real Data Example

Alzheimer's disease (AD) is one of the most common forms of dementia characterized by progressive cognitive and memory deficits. The increasing incidence of AD makes the disease a
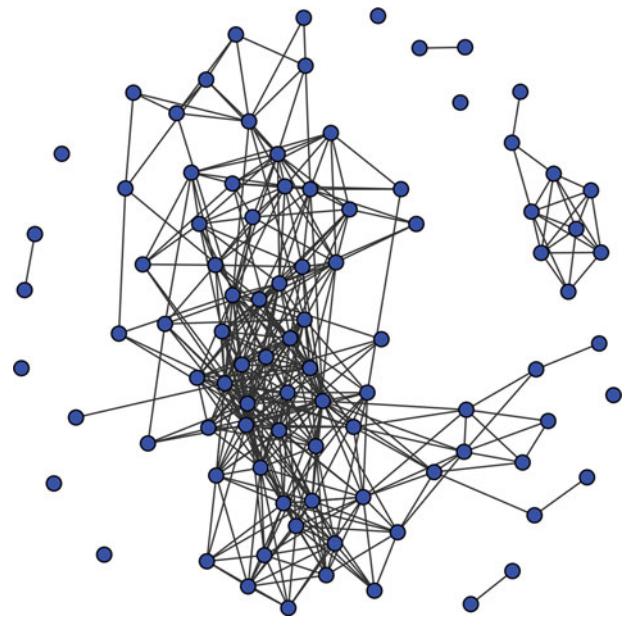

Figure 3. Estimated graph of 93 MRI features.

very important health issue and a huge financial burden for both patients and governments (Hebert et al. 2001). In the practical diagnosis of AD, the Mini Mental State Examination (MMSE) (Folstein, Folstein, and McHugh 1975) score is a very important reference. MMSE is a brief 30-point questionnaire test that is used to screen for cognitive impairment. It can be used to examine patient's arithmetic, memory, and orientation. Generally, any score greater than or equal to 27 points (out of 30) indicates a normal cognition. Below this, MMSE score can indicate severe

Table 8. Time comparison between PD method and IP algorithm.

Examples	n	p	Nedges	p_{new}/p	Time$_{PD}$ (seconds)	Time$_{IP}$ (seconds)
1	40	100	30	1.600	0.083	0.436
2	40	100	99	2.980	0.181	14.850
3	40	100	243	5.860	0.485	44.158
4	400	1500	263229	351.972	277.326	74.701
5	500	2000	475289	476.289	796.735	81.051
6	600	2500	750074	601.059	NA	96.436

NOTE: Nedges: the number of edges in the graph G; p_{new}: the number of predictors in the duplicated predictor matrix; Time$_{PD}$: computing time of the PD method; Time$_{IP}$: computing time of the IP algorithm; NA: out of memory.
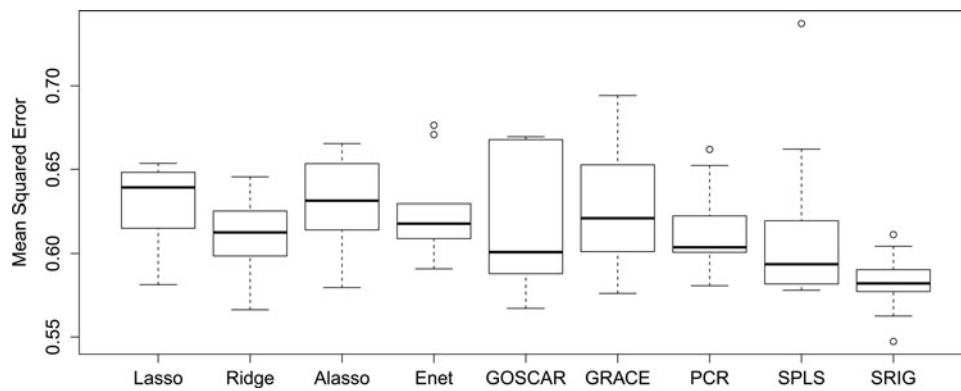
Figure 4. Comparison of MSE for various methods on the ADNI dataset.

(≤9 points), moderate (10–18 points) or mild (19–24 points) cognitive impairment (Mungas 1991). As more and more treatments are being developed and evaluated, it is very important to develop diagnostic and prognostic biomarkers that can predict which individuals are relatively more likely to progress clinically. At present, structural magnetic resonance imaging (MRI) is one of the most popular and powerful techniques for the diagnosis of AD. It is very interesting to use MRI data to predict MMSE score which can be used to diagnose the current disease status of AD.

The dataset we used in this article is the MRI data and MMSE scores of 51 AD patients and 52 normal controls from the Alzheimer's Disease Neuroimaging Initiative (ADNI) database (*www.loni.ucla.edu/ADNI*). The image preprocessing steps for the MRI data include anterior commissure posterior commissure correction, intensity inhomogeneity correction, skull stripping, cerebellum removal, spatial segmentation, and registration. After registration, we obtained the subject-labeled image based a template with 93 manually labeled regions of interest (ROI) (Zhang and Shen 2012). For each of the 93 ROI in the labeled MRI, we computed the volume of GM tissue as a feature. Therefore, the final dataset has 103 subjects. For each subject, there are one MMSE score and 93 MRI features. We treat MMSE score as the response variable and MRI features as predictors in our model.

To evaluate the performance of our proposed SRIG method, we compare it with Lasso, ridge regression, Adaptive Lasso, Elastic net, GOSCAR, GRACE, PCR, and SPLS. The dataset is first scaled to have mean 0 and variance 1 for the MMSE score and each MRI feature. The ten-fold cross-validation (CV) is used to evaluate different methods. The predictor (MRI feature) graph *G* is estimated by the graphical Lasso (Friedman, Hastie, and Tibshirani 2008) only using the training data. Figure 3 shows the estimated MRI feature graph using all the data. There are 93 nodes and 419 edges in this graph. Note that all the models are fitted using training data and evaluated by the mean squared error (MSE) calculated from the testing data. To choose the tuning parameters of different methods, an inner fivefold CV is
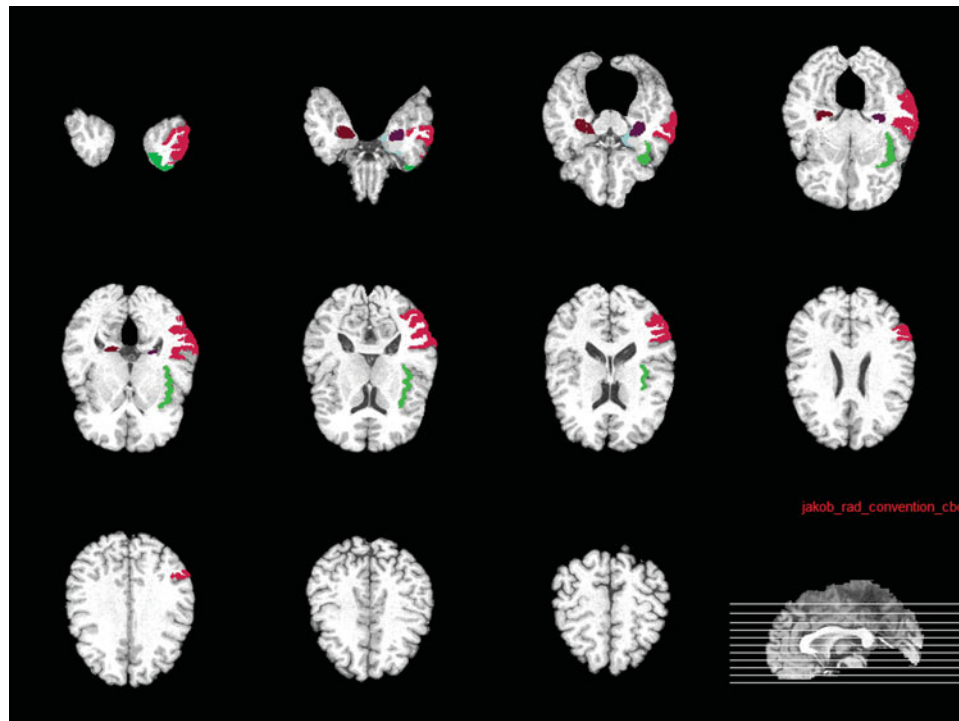
Figure 5. The multislice view of seven brain regions always selected by SRIG method.

used. Considering possible bias due to the random splitting, we repeat 10-CV process 10 times. Figure 4 shows the boxplot of the averaged mean squared errors of different methods. Compared with the other methods, our proposed SRIG method delivers the best prediction of MMSE scores. The averaged MSE acquired by our proposed SRIG method is 0.5822, which is about 4.6% percent lower than the smallest MSE acquired by the competitors.

For the 10 times of our 10-CV process, we acquire 100 models for each method. For our proposed SRIG method, the averaged number of selected MRI features (with estimated coefficients bigger than 0.01) is almost 36. There are seven MRI features always selected by our proposed SRIG method. The feature indices are 4, 19, 22, 30, 69, 80, and 83. Figure 5 shows the multislice view of the brain regions corresponding to these seven MRI features. The colored areas are the selected regions. Interestingly, the 30th and 69th features correspond to the hippocampal regions. The 22th and 83th features correspond to the uncus region and the amygdala region, respectively. These regions are known to be related to AD by many previous studies based on group comparison methods (Jack et al. 1999; Misra, Fan, and Davatzikos 2009; Zhang and Shen 2012). Moreover, we notice that the 4th, 19th, and 80th features relate to the insula right, temporal pole right, and middle temporal gyrus right regions, respectively. It would be very interesting to check whether these regions are substantially related to AD by some group comparison studies.

7. Conclusion

In this article, we propose a new penalized regression method using structure information among predictors. Instead of using the predictor graph *edge-by-edge* as in the existing literature, our proposed SRIG method uses it *node-by-node*. Theoretical study shows that SRIG includes adaptive Lasso, group Lasso, and ridge regression as special cases. It can make use of the general structure information among predictors efficiently. Furthermore, SRIG acquires tight finite sample bounds for both prediction and estimation. It also enjoys the model selection consistency. Both simulation study and real data analysis show that SRIG is a competitive tool for estimation, prediction, and model selection.

Supplementary Materials

The supplementary materials contain technical proofs, additional details on the algorithms discussed in Section 3, case results, and simulation results.

Acknowledgments

Funding

References

Beck, A., and Teboulle, M. (2009), "A Fast Iterative Shrinkage-Thresholding Algorithm for Linear Inverse Problems," *SIAM Journal on Imaging Sciences*, 2, 183–202. [709,710]

Bickel, P. J., Ritov, Y., and Tsybakov, A. B. (2009), "Simultaneous Analysis of Lasso and Dantzig Selector," *The Annals of Statistics*, 37, 1705–1732. [711,712]

Bondell, H. D., and Reich, B. J. (2008), "Simultaneous Regression Shrinkage, Variable Selection, and Supervised Clustering of Predictors With OSCAR," *Biometrics*, 64, 115–123. [708]

Breheny, P., and Huang, J. (2009), "Penalized Methods for Bi-Level Variable Selection," *Statistics and Its Interface*, 2, 369–380. [709]

Cai, T., Liu, W., and Luo, X. (2011), "A Constrained l_1 Minimization Approach to Sparse Precision Matrix Estimation," *Journal of the American Statistical Association*, 106, 594–607. [707,713]

Chung, D., Chun, H., and Keles, S. (2012), "Spls: Sparse Partial Least Squares (SPLS) Regression and Classification," *R package, version*, 2, 1–1. [713]

Combettes, P. L., and Pesquet, J.-C. (2011), "Proximal Splitting Methods in Signal Processing," *Fixed-Point Algorithms for Inverse Problems in Science and Engineering*, pp. 185–212, Berlin: Springer. [710]

Fan, J., and Li, R. (2001), "Variable Selection via Nonconcave Penalized Likelihood and its Oracle Properties," *Journal of the American Statistical Association*, 96, 1348–1361. [707]

Folstein, M. F., Folstein, S. E., and McHugh, P. R. (1975), "Mini-Mental State: A Practical Method for Grading the Cognitive State of Patients for the Clinician," *Journal of Psychiatric Research*, 12, 189–198. [708,717]

Friedman, J., Hastie, T., and Tibshirani, R. (2008), "Sparse Inverse Covariance Estimation With the Graphical Lasso," *Biostatistics*, 9, 432–441. [707,713,718]

Greenshtein, E. (2006), "Best Subset Selection, Persistence in High-Dimensional Statistical Learning and Optimization Under l1 Constraint," *The Annals of Statistics*, 34, 2367–2386. [707]

Hebert, L. E., Beckett, L. A., Scherr, P. A., and Evans, D. A. (2001), "Annual Incidence of Alzheimer Disease in the United States Projected to the Years 2000 Through 2050," *Alzheimer Disease & Associated Disorders*, 15, 169–173. [717]

Hoerl, A. E., and Kennard, R. W. (1970), "Ridge Regression: Biased Estimation for Nonorthogonal Problems," *Technometrics*, 12, 55–67. [707]

Jack, C., Petersen, R. C., Xu, Y. C., O'Brien, P. C., Smith, G. E., Ivnik, R. J., Boeve, B. F., Waring, S. C., Tangalos, E. G., and Kokmen, E. (1999), "Prediction of AD With MRI-Based Hippocampal Volume in Mild Cognitive Impairment," *Neurology*, 52, 1397–1397. [719]

Kim, S., Pan, W., and Shen, X. (2013), "Network-Based Penalized Regression With Application to Genomic Data," *Biometrics*, 69, 582–593. [708]

Kim, S., and Xing, E. P. (2009), "Statistical Estimation of Correlated Genome Associations to a Quantitative Trait Network," *PLoS Genetics*, 5, e1000587. [708]

Knight, K., and Fu, W. (2000), "Asymptotics for Lasso-Type Estimators," *Annals of Statistics*, 1356–1378. [707]

Li, C., and Li, H. (2008), "Network-Constrained Regularization and Variable Selection for Analysis of Genomic Data," *Bioinformatics*, 24, 1175–1182. [707,713]

Liu, Y., and Wu, Y. (2007), "Variable Selection via a Combination of the L0 and L1 Penalties," *Journal of Computational and Graphical Statistics*, 16, 782–798. [707]

Lounici, K., Pontil, M., Geer, S., Tsybakov, A. B., et al. (2011), "Oracle Inequalities and Optimal Inference Under Group Sparsity," *The Annals of Statistics*, 39, 2164–2204. [711]

Mevik, B.-H., and Wehrens, R. (2007), "The pls Package: Principal Component and Partial Least Squares Regression in R," *Journal of Statistical Software*, 18, 1–24. [713]

Misra, C., Fan, Y., and Davatzikos, C. (2009), "Baseline and Longitudinal Patterns of Brain Atrophy in MCI Patients, and Their use in Prediction

of Short-Term Conversion to AD: Results From ADNI," *NeuroImage*, 44, 1414–1422. [719]

Mungas, D. (1991), "In-Office Mental Status Testing: A Practical Guide," *Geriatrics*, 46, 54–66. [718]

Nardi, Y., and Rinaldo, A. (2008), "On the Asymptotic Properties of the Group Lasso Estimator for Linear Models," *Electronic Journal of Statistics*, 2, 605–633. [710,711]

Obozinski, G., Jacob, L., and Vert, J.-P. (2011), "Group Lasso With Overlaps: the Latent Group Lasso Approach," *arXiv preprint arXiv:1110.0413*. [708,709,710]

Pan, W., Xie, B., and Shen, X. (2010), "Incorporating Predictor Network in Penalized Regression With Application to Microarray Data," *Biometrics*, 66, 474–484. [708]

Percival, D. (2012), "Theoretical Properties of the Overlapping Groups Lasso," *Electronic Journal of Statistics*, 6, 269–288. [711]

Subramanian, A., Tamayo, P., Mootha, V. K., Mukherjee, S., Ebert, B. L., Gillette, M. A., Paulovich, A., Pomeroy, S. L., Golub, T. R., Lander, E. S., et al. (2005), "Gene Set Enrichment Analysis: A Knowledge-Based Approach for Interpreting Genome-Wide Expression Profiles," *Proceedings of the National Academy of Sciences of the United States of America*, 102, 15545–15550. [707]

Tibshirani, R. (1996), "Regression Shrinkage and Selection via the Lasso," *Journal of the Royal Statistical Society*, Series B, 58, 267–288. [707]

Villa, S., Rosasco, L., Mosci, S., and Verri, A. (2014), "Proximal Methods for the Latent Group Lasso Penalty," *Computational Optimization and Applications*, 58, 381–407. [710]

Wang, H., Li, G., and Jiang, G. (2007), "Robust Regression Shrinkage and Consistent Variable Selection Through the LAD-Lasso," *Journal of Business & Economic Statistics*, 25, 347–355. [707]

Witten, D. M., and Tibshirani, R. (2009), "Covariance-Regularized Regression and Classification for High Dimensional Problems," *Journal of the Royal Statistical Society*, Series B, 71, 615–636. [707]

Yang, S., Yuan, L., Lai, Y.-C., Shen, X., Wonka, P., and Ye, J. (2012), "Feature Grouping and Selection Over an Undirected Graph," *Proceedings of the 18th ACM SIGKDD International Conference on Knowledge Discovery and Data Mining*, ACM, pp. 922–930. [708,713]

Yang, Y., and Zou, H. (2013), *gglasso: Group Lasso Penalized Learning Using A Unified BMD Algorithm*, r package version 1.1. [709]

Yuan, M., and Lin, Y. (2006), "Model Selection and Estimation in Regression With Grouped Variables," *Journal of the Royal Statistical Society*, Series B, 68, 49–67. [707]

—— (2007), "Model Selection and Estimation in the Gaussian Graphical Model," *Biometrika*, 94, 19–35. [707]

Zhang, C.-H. (2010), "Nearly Unbiased Variable Selection Under Minimax Concave Penalty," *The Annals of Statistics*, 38, 894–942. [707]

Zhang, D., and Shen, D. (2012), "Multi-Modal Multi-Task Learning for Joint Prediction of Multiple Regression and Classification Variables in Alzheimer's Disease," *NeuroImage*, 59, 895–907. [718,719]

Zhang, W., Wan, Y.-W., Allen, G. I., Pang, K., Anderson, M. L., and Liu, Z. (2013), "Molecular Pathway Identification Using Biological Network-Regularized Logistic Models," *BMC Genomics*, 14, S7. [708]

Zhao, P., and Yu, B. (2006), "On Model Selection Consistency of Lasso," *The Journal of Machine Learning Research*, 7, 2541–2563. [707,712]

Zhou, S., van de Geer, S., and Bühlmann, P. (2009), "Adaptive Lasso for High Dimensional Regression and Gaussian Graphical Modeling," *arXiv preprint arXiv:0903.2515*. [712]

Zhu, Y., Shen, X., and Pan, W. (2013), "Simultaneous Grouping Pursuit and Feature Selection Over an Undirected Graph," *Journal of the American Statistical Association*, 108, 713–725. [708]

Zou, H. (2006), "The Adaptive Lasso and its Oracle Properties," *Journal of the American Statistical Association*, 101, 1418–1429. [707,711]

Zou, H., and Hastie, T. (2005), "Regularization and Variable Selection via the Elastic Net," *Journal of the Royal Statistical Society*, Series B, 67, 301–320. [707]